

The Hamiltonian particle-mesh method for the spherical shallow water equations

J. Frank^{1*} and S. Reich²

¹CWI, Amsterdam, The Netherlands

²Department of Mathematics, Imperial College London, London, UK

*Correspondence to:

J. Frank, CWI, P.O. Box 94079,

1090 GB Amsterdam, The

Netherlands.

E-mail: jason@cwi.nl

Abstract

The Hamiltonian particle-mesh (HPM) method is generalized to the spherical shallow-water equations, utilizing constrained particle dynamics on the sphere and Merilees pseudospectral method (complexity $\mathcal{O}(J^2 \log J)$ in the latitudinal gridsize) to approximate the inverse modified Helmholtz regularization operator. The time step for the explicit, symplectic integrator depends only on a uniform physical smoothing length. Copyright © 2004 Royal Meteorological Society

Keywords: shallow-water equations; spherical geometry; particle-mesh method; Hamiltonian equations of motion; constraints; symplectic integration

Received: 12 December 2003

Revised: 27 February 2003

Accepted: 15 March 2003

1. Introduction

In this paper, we extend the Hamiltonian particle-mesh (HPM) method of Frank and Reich (2003) and Frank *et al.* (2002) to the shallow-water equations in spherical geometry (Williamson *et al.* 1992). By working with a fully Lagrangian description, and embedding the sphere in \mathbb{R}^3 , one can avoid pole-related step-size limitations and retain exact conservation of mass, energy and circulation. Additionally, the method can be made symplectic, which has even stronger implications, and in particular implies conservation of potential vorticity. We take Côte's (1988) three-dimensional constrained formulation

$$\begin{aligned}\frac{d}{dt}\mathbf{x} &= \mathbf{v}, \\ \frac{d}{dt}\mathbf{v} &= -2\Omega\mathbf{k} \times \mathbf{v} - g\nabla_x h - \lambda\mathbf{x}, \\ 0 &= \mathbf{x} \cdot \mathbf{x} - R^2\end{aligned}$$

as a starting point to derive an approximation to the shallow-water equations in the form of a constrained system of ordinary differential equations (ODEs) in the particle positions \mathbf{x}_k and their velocities \mathbf{v}_k , $k = 1, \dots, K$. Here $g = 9.80616 \text{ m s}^{-2}$ is the gravitational constant, $\Omega = 7.292 \times 10^{-5} \text{ s}^{-1}$ is the rotation rate of the earth, $R = 6.37122 \times 10^6 \text{ m}$ is the radius of the earth, h is the geopotential layer depth, $\mathbf{k} = (0, 0, 1)^T$, and λ is a Lagrange multiplier to enforce the position constraint.

A key aspect of the HPM method is the regularization or smoothing of the particle-based discrete mass distribution over a computational grid, which yields the layer depth. The regularization is a differential operator: specifically, an inverse modified Helmholtz operator. In the present paper we approximate the

Helmholtz operator using a directional splitting and utilize a spectral technique due to Merilees (1973) to approximate differential operators and their inverses over the sphere. Merilees method uses FFTs in both longitudinal and latitudinal directions and requires $\mathcal{O}(J^2 \log J)$ operations per smoothing step as opposed to $\mathcal{O}(J^3)$ operations for the spectral transform method (see Spatz *et al.* 1998). Here J denotes the number of grid points in the latitudinal direction. We note that for very fine discretizations, or in a parallel computing environment, the FFT-based smoother may be replaced by a gridpoint-based approximation without significantly influencing our results.

Another key aspect of the HPM method lies in the variational or Hamiltonian nature of the spatial truncation. This property, combined with a symplectic time-stepping algorithm (Hairer *et al.* 2002), guarantees excellent conservation of total energy and circulation (Frank and Reich, 2003). These desirable properties also apply to the proposed HPM in spherical geometry and we demonstrate this for a numerical test problem from Williamson *et al.* (1992). Finally, the time steps achievable for our semi-explicit symplectic integration method are entirely determined by the uniform physical smoothing length and not by the longitude–latitude gridsize near the poles.

2. Description of the spatial truncation

The HPM method utilizes a set of K particles with coordinates $\mathbf{x}_k \in \mathbb{R}^3$ and velocities $\mathbf{v}_k \in \mathbb{R}^3$ as well as a *longitude–latitude grid* with equal grid spacing $\Delta\lambda = \Delta\theta = \pi/J$. The latitude grid points are offset a half-grid length from the poles. Hence we obtain grid points (λ_m, θ_n) , where $\lambda_m = m\Delta\lambda$, $\theta_n = -\frac{\pi}{2} +$

$(n - 1/2)\Delta\theta$, $m = 1, \dots, 2J$, $n = 1, \dots, J$, and the grid dimension is $2J \times J$.

All particle positions satisfy the holonomic constraint

$$\mathbf{x}_k \cdot \mathbf{x}_k = R^2 \quad (1)$$

where $R > 0$ is the radius of the sphere. Differentiating the constraint (1) with respect to time immediately implies the velocity constraint

$$\mathbf{x}_k \cdot \mathbf{v}_k = 0 \quad (2)$$

We convert between *Cartesian* and *spherical coordinates* using the formulas

$$x = R \cos \lambda \cos \theta, \quad y = R \sin \lambda \cos \theta, \quad z = R \sin \theta$$

and

$$\lambda = \tan^{-1} \left(\frac{y}{x} \right), \quad \theta = \sin^{-1} \left(\frac{z}{R} \right)$$

Hence we associate with each particle position $\mathbf{x}_k = (x_k, y_k, z_k)^T$ a spherical coordinate (λ_k, θ_k) .

The implementation of the HPM method is greatly simplified by making use of the *periodicity* of the spherical coordinate system in the following sense. The periodicity is trivial in the longitudinal direction. For the latitude, a great circle meridian is formed by connecting the latitude data separated by an angular distance π in longitude (or J grid points). See, for example, the paper by Spetz *et al.* (1998).

Let $\psi^{mn}(\mathbf{x})$ denote the *tensor product cubic B-spline* centred at a grid point (λ_m, θ_n) , ie

$$\psi^{mn}(\mathbf{x}) \equiv \psi_{cs} \left(\frac{\lambda - \lambda_m}{\Delta\lambda} \right) \cdot \psi_{cs} \left(\frac{\theta - \theta_n}{\Delta\theta} \right) \quad (3)$$

where $\psi_{cs}(r)$ is the cubic spline

$$\psi_{cs}(r) \equiv \begin{cases} \frac{2}{3} - |r|^2 + \frac{1}{2}|r|^3, & |r| \leq 1, \\ \frac{1}{6}(2 - |r|)^3, & 1 < |r| \leq 2, \\ 0, & |r| > 2 \end{cases}$$

and (λ, θ) are the spherical coordinates of a point \mathbf{x} on the sphere.

In evaluating Equation (3) it is understood that the distances $\lambda - \lambda_m$ and $\theta - \theta_n$ are taken as the minimum over all periodic images of the arguments. With this convention the basis functions form a *partition of unity*, ie

$$\sum_{m,n} \psi^{mn}(\mathbf{x}) = 1 \quad (4)$$

hence satisfying a minimum requirement for approximation from the grid to the rest of the sphere.

The gradient of $\psi^{mn}(\mathbf{x})$ in \mathbb{R}^3 can be computed using the chain rule and the standard formula

$$\nabla_{\mathbf{x}} = \frac{1}{R} \hat{\boldsymbol{\theta}} \frac{\partial}{\partial \theta} + \frac{1}{R \cos \theta} \hat{\boldsymbol{\lambda}} \frac{\partial}{\partial \lambda}$$

with unit vectors

$$\hat{\boldsymbol{\theta}} = \begin{bmatrix} -\cos \lambda \sin \theta \\ -\sin \lambda \sin \theta \\ \cos \theta \end{bmatrix}, \quad \hat{\boldsymbol{\lambda}} = \begin{bmatrix} -\sin \lambda \\ \cos \lambda \\ 0 \end{bmatrix}$$

Let us assume for a moment that we have computed a layer depth approximation $\hat{H}_{mn}(t)$ over the longitude–latitude grid. Making use of the partition of unity (4), a continuous layer depth approximation is obtained:

$$\hat{h}(\mathbf{x}, t) = \sum_{mn} \hat{H}_{mn} \psi^{mn}(\mathbf{x}) \quad (5)$$

Computing the gradient of this approximation at particle positions \mathbf{x}_k , the Newtonian equations of motion for each particle on the sphere are given by the constrained formulation

$$\frac{d}{dt} \mathbf{x}_k = \mathbf{v}_k, \quad (6)$$

$$\frac{d}{dt} \mathbf{v}_k = -2\Omega \mathbf{k} \times \mathbf{v}_k - g \sum_{m,n} \nabla_{\mathbf{x}_k} \psi^{mn}(\mathbf{x}_k)$$

$$\times \hat{H}_{mn}(t) - \lambda_k \mathbf{x}_k, \quad (7)$$

$$0 = \mathbf{x}_k \cdot \mathbf{x}_k - R^2 \quad (8)$$

To close the equations of motion, we define the geopotential layer depth $\hat{H}_{mn}(t)$ as follows. We assign to each particle a fixed mass m_k which represents its local contribution to the layer depth approximation and essentially equidistribute the particles (in the physical metric) over the sphere at the initial time $t = 0$. First, we compute

$$A_{mn} = \sum_k \psi^{mn}(\mathbf{x}_k). \quad (9)$$

We find that A_{mn} is not approximately constant but rather

$$A_{mn} \approx \cos(\theta_n) \cdot \text{const}$$

ie, A_{mn} is proportional to the area of the associated longitude–latitude grid cell on the sphere. Second, we define the particle masses

$$m_k = \sum_{m,n} H_{mn} \psi^{mn}(\mathbf{x}_k) \quad (10)$$

and obtain

$$H_{mn} \approx \frac{1}{A_{mn}} \sum_k m_k \psi^{mn}(\mathbf{x}_k)$$

which provides us with the desired layer depth approximation. The area coefficients (9) and the particle masses (10) are only computed once at the beginning of the simulation. During the simulation the layer

depth is approximated over the longitude–latitude grid using the formula

$$H_{mn}(t) = \frac{1}{A_{mn}} \sum_k m_k \psi^{mn}(\mathbf{x}_k(t)) \quad (11)$$

A crucial step in the development of an HPM method is the implementation of an appropriate smoothing operator \mathbf{S} over the longitude–latitude grid. We will derive such a smoothing operator in the subsequent section. For now we simply assume the existence of a symmetric linear operator \mathbf{S} and define smoothed grid functions via $\mathbf{S} : \{A_{mn}\} \rightarrow \{\tilde{A}_{mn}\}$ and $\mathbf{S} : \{M_{mn}\} \rightarrow \{\tilde{M}_{mn}\}$, respectively, where

$$M_{mn}(t) = \sum_k m_k \psi^{mn}(\mathbf{x}_k(t))$$

We now replace the definition (11) by

$$\tilde{H}_{mn}(t) = \frac{\tilde{M}_{mn}(t)}{\tilde{A}_{mn}} \quad (12)$$

and finally introduce $\hat{H}_{mn}(t)$ via $\mathbf{S} : \{\tilde{H}_{mn}\} \rightarrow \{\hat{H}_{mn}\}$. This approximation is used in Equation (7) and closes the equations of motion.

2.1. Conservation properties

The HPM method conserves mass, energy, symplectic structure, circulation, potential vorticity and geostrophic balance.

Trivially, since the *mass* associated with each particle is fixed for the entire integration, the HPM method has local and total mass conservation. Furthermore, Equation (4) implies $d/dt \sum_{m,n} M_{m,n} = 0$, and the same will hold for $\tilde{M}_{mn}(t)$ for appropriate \mathbf{S} . This implies the conservation of $\sum_{mn} \tilde{H}_{mn}(t) \tilde{A}_{mn}$ by Equation (12).

Since the HPM particles are accelerated in the exact gradient field of Equation (5), one can define an auxiliary continuum fluid whose particle and velocity fields initially interpolate the $\mathbf{x}_k(0)$ and $\mathbf{u}_k(0)$, evolve this fluid under the continuous approximate layer depth (5), and the HPM method will *remain embedded in the auxiliary flow*.

In Frank and Reich (2003) we show that the auxiliary fluid satisfies a *circulation theorem* and, via ‘Stokes’ theorem, conserves vorticity. The auxiliary fluid also conserves *potential vorticity*, and this permits us to approximate PV by simply assigning the PV of the auxiliary fluid to the particles, ie $q_k(0) = q(\mathbf{x}_k, 0)$, and advecting this with the particles. Generalized potential enstrophy conservation follows when a function $f(q)$ is approximated in a manner analogous to Equations (5) and (11). See Frank and Reich (2003) for full details.

The equations of motion (6) — (8) define a constrained Hamiltonian system that conserves the *total energy* (Hamiltonian)

$$\mathcal{H} = \sum_k \frac{m_k}{2} \mathbf{v}_k \cdot \mathbf{v}_k + \frac{g}{2} \sum_{m,n} \tilde{H}_{mn}^2 \tilde{A}_{mn}.$$

Note that $\tilde{H}_{mn}^2 \tilde{A}_{mn} = \tilde{M}_{mn}^2 \tilde{A}_{mn}^{-1}$. The *symplectic structure* of phase space is given by

$$\omega = \sum_k m_k d\mathbf{v}_k \wedge \mathbf{x}_k + \Omega \sum_k m_k d\mathbf{x}_k \wedge (\mathbf{k} \times d\mathbf{x}_k) \quad (13)$$

The symplectic structure may be also embedded the auxiliary fluid, allowing one to pull back to label space by writing the particle flow as a function of the initial conditions. One consequence of this is another statement of potential vorticity conservation. See Bridges *et al.* (2004) for a discussion of symplecticity and PV. See also Cotter and Reich (2004) for a discussion of the preservation properties of HPM for *adiabatic invariants* and the implications of this for geostrophic and (in vertical or 3D models) hydrostatic balance relations.

3. The smoothing operator

To complete the description of the HPM method, we need to find an inexpensive smoothing operator that averages out fluctuations over the sphere on some length scale Λ . Following Merilees’ pseudospectral code (Merilees, 1973), we compute derivatives by employing one-dimensional fast Fourier transforms (FFTs) along the longitudinal and the latitudinal directions as summarized, for example, by Fornberg (1995) and Spatz *et al.* (1998). This allows us essentially to follow the HPM smoothing approach of Frank and Reich (2003) and Frank *et al.* (2002), which achieves smoothing by inverting a modified Helmholtz operator $\mathbb{H}(\Lambda^2) = 1 - \Lambda^2 \nabla_x^2$ using two-dimensional FFT over a regular grid in planar geometry. More specifically, one can easily solve modified Helmholtz equations separately in the longitudinal and latitudinal directions and apply an operator-splitting idea to define a two-dimensional smoothing operator. The key observation is that such a smoothing operator is cheaper to implement than the inversion of a modified Helmholtz operator using spherical harmonics. We would like to mention that our smoothing operator is different from the filtering achieved in the pseudospectral method of Spatz *et al.* (1998), which is needed to control aliasing in a pseudospectral method.

We use the following specific technique to achieve approximately uniform smoothing over the sphere with a physical smoothing length Λ . In the lateral direction we use the modified Helmholtz operator

$$\mathbb{H}_{\text{lat}}(\Lambda^2) = 1 - \frac{\Lambda^2}{R^2} \frac{\partial^2}{\partial \theta^2}$$

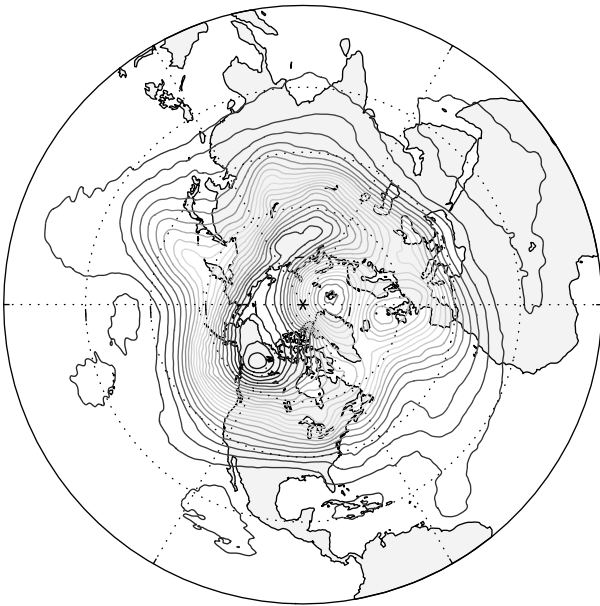


Figure 1. Stereographic projection of 500 mb geopotential height field on day 5, Test case 7. Contours by 50 m from 9050 (blue) to 10250 (red) A movie is available from the [supplementary materials](#) page

In the longitudinal direction a uniform physical smoothing length is obtained with

$$\mathbb{H}_{\text{lon}}(\Lambda^2) = 1 - \frac{\Lambda^2}{R^2 \cos^2 \theta} \frac{\partial^2}{\partial \lambda^2}$$

and, using a second-order operator splitting, the complete smoothing operator can schematically be written as

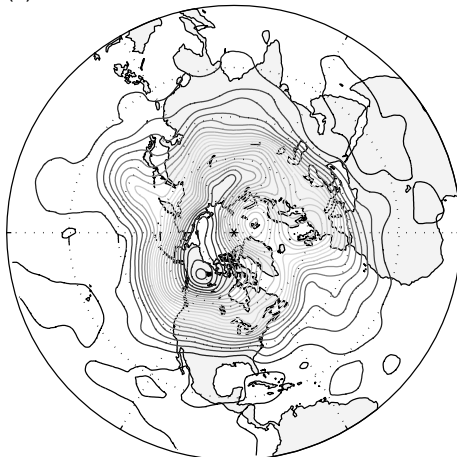
$$\mathbb{S} = \mathbb{H}_{\text{lon}}^{-1}(\Lambda^2/2) \circ \mathbb{H}_{\text{lat}}^{-1}(\Lambda^2) \circ \mathbb{H}_{\text{lon}}^{-1}(\Lambda^2/2)$$

Upon implementing these operators using FFTs, we obtain a discrete approximation \mathbb{S} over the longitude–latitude grid which was used in the previous section to define the layer depth \hat{H}_{mn} .

4. Time discretization and numerical experiments

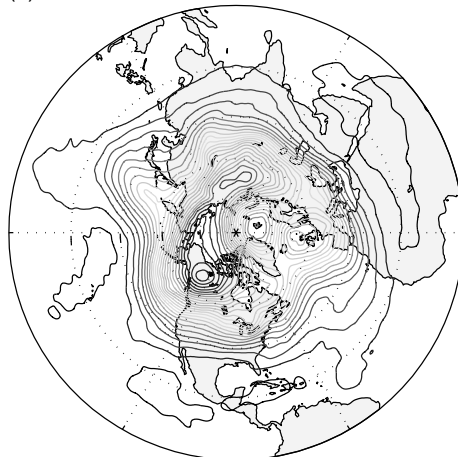
Since the equations of motion (6)–(8) are Hamiltonian, it is desirable to integrate them with a symplectic

(a) $J=128$



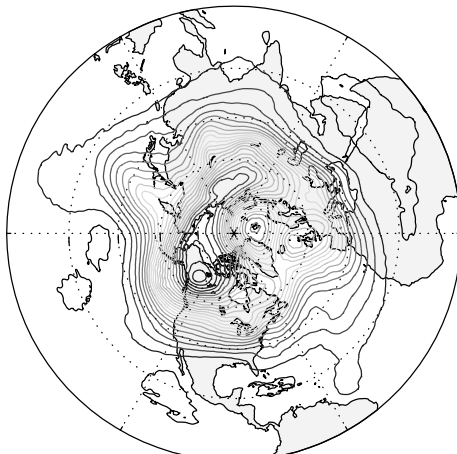
contour from 9050 to 10250 by 50

(b) $J=256$



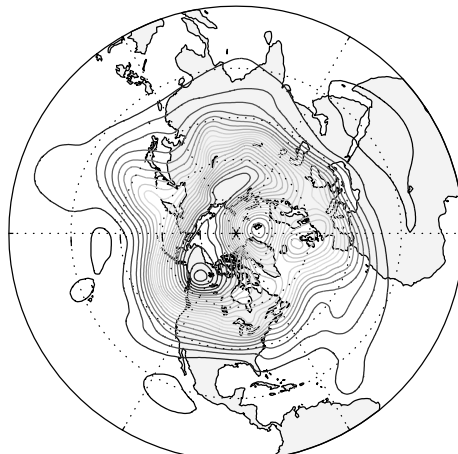
contour from 9050 to 10250 by 50

(c) $J=384$



contour from 9050 to 10250 by 50

(d)



contour from 9050 to 10250 by 50

Figure 2. Comparison of Day 5 solution for (a) $J = 128$, (b) $J = 256$, (c) $J = 384$, (d) T213 reference solution

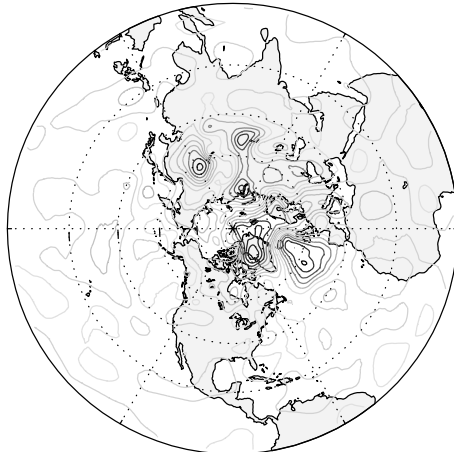
method, as this implies long-time approximate conservation of energy, symplectic structure (and hence PV) and adiabatic invariants such as geostrophic balance. Therefore, the following modification of the symplectic RATTLE/SHAKE algorithm (Hairer *et al.* 2002) suggests itself:

$$\begin{aligned} \mathbf{v}_k^{n+1/2} &= (\mathbf{I} + \Delta t \Omega \mathbf{k} \times)^{-1} \left[\mathbf{v}_k^n - \frac{g \Delta t}{2} \right. \\ &\quad \left. \times \nabla_{\mathbf{x}_k} \sum_{m,n} \psi^{mn}(\mathbf{x}_k^n) \hat{H}_{mn}(t_n) - \lambda_k^n \mathbf{x}_k^n \right], \\ \mathbf{x}_k^{n+1} &= \mathbf{x}_k^n + \Delta t \mathbf{v}_k^{n+1/2} \\ 0 &= \mathbf{x}_k^{n+1} \cdot \mathbf{x}_k^{n+1} - R^2, \\ \bar{\mathbf{v}}_k^{n+1} &= (\mathbf{I} - \Delta t \Omega \mathbf{k} \times) \mathbf{v}_k^{n+1/2} - \frac{g \Delta t}{2} \\ &\quad \times \nabla_{\mathbf{x}_k} \sum_{m,n} \psi^{mn}(\mathbf{x}_k^{n+1}) \hat{H}_{mn}(t_{n+1}), \\ \mathbf{v}_k^{n+1} &= \bar{\mathbf{v}}_k^{n+1} - R^{-2} \mathbf{x}_k(\mathbf{x}_k^{n+1} \cdot \bar{\mathbf{v}}_k^{n+1}) \end{aligned}$$

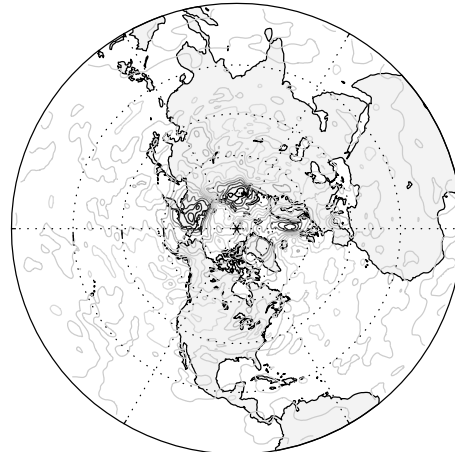
The first three equations, solved simultaneously, lead to a scalar quadratic equation in the Lagrange multiplier λ_k^n for each k . The roots correspond to projecting the particle to the near and far sides of the sphere, so the smallest root is taken. The last two equations update the velocity field and enforce Equation (2). Hence the above time-stepping method is explicit. One can show that the method also conserves the symplectic two form (13) and hence is symplectic (Hairer *et al.* 2002).

To validate the HPM method, we integrated Test Case 7 (Analyzed 500 mb Height and Wind Field Initial Conditions) from Williamson *et al.* (1992) with the initial data of 21 December 1978 (T213 truncation), over an interval of 5 days. All calculations were done in Matlab, using *mex* extensions in C for particle-mesh operators. We have observed no significant, long-lived clustering of particles.

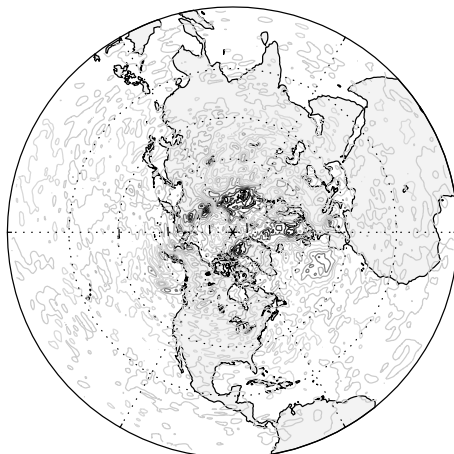
The discretization parameters (number of latitudinal gridpoints J , total number of particles K , smoothing length Λ , and time step size of Δt) for the various

 (a) $J=128$


contour from -200 to 200 by 25

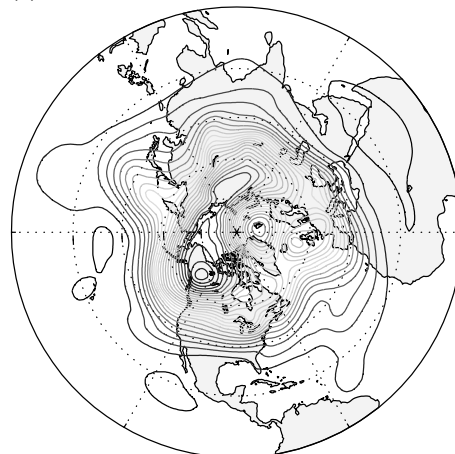
 (b) $J=256$


contour from -100 to 100 by 12.5

 (c) $J=384$


contour from -50 to 50 by 6.25

(d)



contour from 9050 to 10250 by 50

Figure 3. Stereographic projection of error in geopotential on day 5 for (a) $J = 128$, (b) $J = 256$ and (c) $J = 384$. The reference solution is reproduced in (d)

runs are listed in the table below:

| J | K | $\Lambda(m)$ | $\Delta t(s)$ |
|-----|-----------|----------------------|---------------|
| 128 | 333 758 | 3.1275×10^5 | 1728 |
| 256 | 1 335 096 | 1.5637×10^5 | 864 |
| 384 | 3 003 976 | 1.0425×10^5 | 432 |

A stereographic projection of the geopotential field in the Northern Hemisphere is shown in Figure 1 for the $J = 384$ simulation, and agrees quite well with the solution shown in Figure 5.13 of Jakob-Chien *et al.* (1995). In Figure 2 we give a comparison of the solutions obtained for $J = 128$, $J = 256$, and $J = 384$

with the T213 reference solution.¹ The error in the geopotential fields for these same cases is compared in Figure 3. The reader will note that there is an error in the geopotential at time $t = 0$ already. This error is due to the fact that the geopotential is determined by the particle masses m_k . The mass coefficients are assigned initially with a certain approximation error. As a result, small-scale gravity waves may be present in the initial

¹The reference solution was computed using the spectral transform method and Gaussian quadrature points in the latitudinal direction (Jakob-Chien *et al.* 1995). A least squares extrapolation of the ℓ_2 errors reported in Jakob-Chien *et al.* (1995), assuming just polynomial convergence of the spectral method, predicts an error of 5×10^{-4} for the T213 truncation.

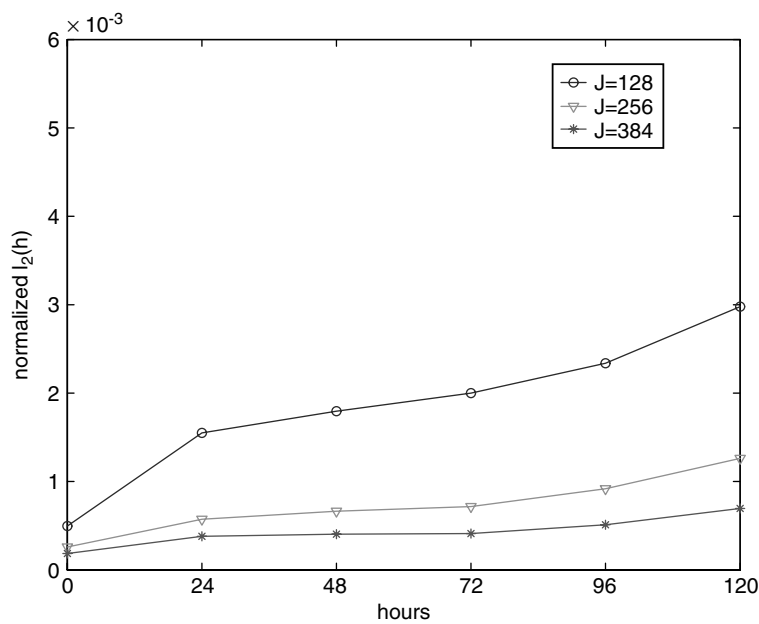


Figure 4. Error growth in the ℓ_2 -norm of the geopotential height field

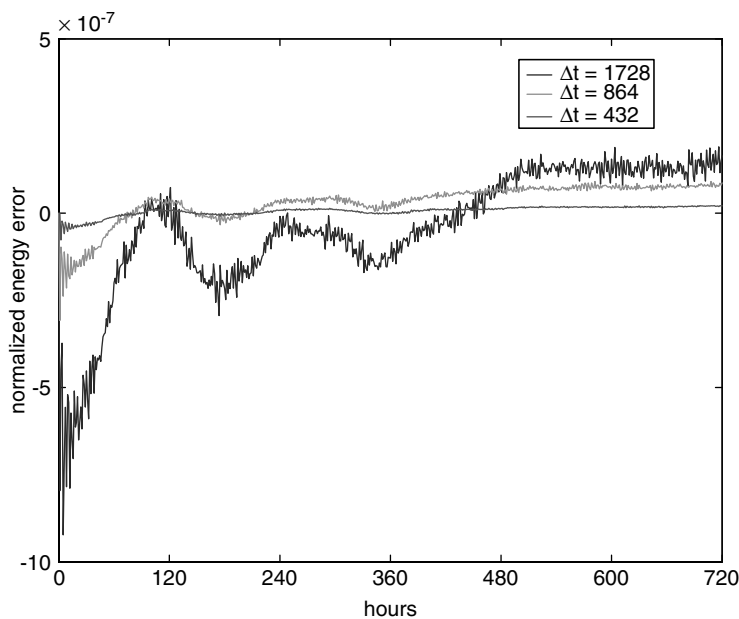


Figure 5. Variation in total energy over a 30-day simulation

state, even though these have been filtered out of the reference data. These unbalanced gravity waves also account for the fine-scale fluctuations observed in Figure 1.

Figure 4 shows the growth of error in the ℓ_2 -norm for the geopotential height over the 5-day period, for $J = 128$, $J = 256$ and $J = 384$. We observe approximately first-order convergence. (A numerical approximation of the order exponent based on the given data gave $p \approx 1.3$.) We attribute the low-order convergence to the complex dynamics of this test case. Higher-order convergence would be expected for other test cases from Williamson *et al.* (1992).

As pointed out in Section 2, mass and potential enstrophy are preserved to machine precision by the HPM method. Figure 5 illustrates the energy conservation property of the HPM method. For this simulation, we chose a coarse discretization of $J = 128$, and integrated over a long interval of 30 days using step sizes of $\Delta t = 432$ sec, $\Delta t = 864$ sec and $\Delta t = 1728$ sec. The relative energy errors observed at day 30 were 2.0859×10^{-8} , 8.667×10^{-8} and 1.645×10^{-7} , respectively. Note the relatively large errors right at the beginning of the simulation. These are due to the imbalance of the numerical initial data and the rapid subsequent adjustment process.

Acknowledgments

J. Frank is funded by an Innovative Research Grant from the Netherlands Organization for Scientific Research (NWO). S. Reich acknowledges partial financial support by EPSRC Grant GR/R09565/01.

References

- Bridges TJ, Hydon P, Reich S. 2004. Vorticity and symplecticity in Lagrangian fluid dynamics. *Proceedings of the Royal Society of London* (submitted).
- Côte J. 1988. A Lagrange multiplier approach for the metric terms of semi-Lagrangian models on the sphere. *Quarterly Journal of the Royal Meteorological Society* **114**: 1347–1352.
- Cotter CJ, Reich S. 2004. Adiabatic invariance and applications to MD and NWP. *BIT* (to appear).
- Fornberg B. 1995. A pseudospectral approach for polar and spherical geometrics, *SIAM Journal on Scientific Computing* **16**: 1071–1081.
- Frank J, Reich S. 2003. Conservation properties of smoothed particle hydrodynamics applied to the shallow water equations. *BIT* **43**: 40–54.
- Frank J, Gottwald G, Reich S. 2002. A Hamiltonian particle-mesh method for the rotating shallow-water equations. In *Lecture Notes in Computational Science and Engineering*, vol. 26 Springer: Heidelberg, 131–142.
- Hairer E, Lubich C, Wanner G. 2002. *Geometric Numerical Integration: Structure-Preserving Algorithms for Ordinary Differential Equations*. Springer: Heidelberg.
- Jakob-Chien R, Hack JJ, Williamson DL. 1995. Spectral transform solutions to the shallow water test set. *Journal of Computational Physics* **119**: 164–187.
- Merilees PE. 1973. The pseudospectral approximation applied to the shallow water equations on the sphere. *Atmosphere* **11**: 13–20.
- Spotz WF, Taylor MA, Swarztrauber PN. 1998. Fast shallow-water equations solvers in latitude–longitude coordinates. *Journal of Computational Physics* **145**: 432–444.
- Williamson DL, Drake JB, Hack JJ, Jakob R, Swarztrauber PN. 1992. A standard test set for the numerical approximations to the shallow water equations in spherical geometry. *Journal of Computational Physics* **102**: 211–224.